Visually guided behaviours in Zebrafish larvae and the role of Fmn2b

A Thesis

submitted to

Indian Institute of Science Education and Research Pune in partial fulfilment of the requirements for the BS-MS Dual Degree Programme

by

Antony Kiran K David



Indian Institute of Science Education and Research Pune

Dr. Homi Bhabha Road,

Pashan, Pune 411008, INDIA.

Date: April 2023

Under the guidance of

Supervisor: Dr Aurnab Ghose,

Professor, Department of Biology, IISER Pune

From May 2022 to Mar 2023

INDIAN INSTITUTE OF SCIENCE EDUCATION AND RESEARCH PUNE

Certificate

This is to certify that this dissertation entitled **Visually guided behaviours in Zebrafish larvae and the role of Fmn2b** towards the partial fulfilment of the BS-MS dual degree programme at the Indian Institute of Science Education and Research, Pune represents study/work carried out by **Antony Kiran K David** at Indian Institute of Science Education and Research under the supervision of **Dr Aurnab Ghose**, Professor, Department of Biology, during the academic year 2022-2023.



Dr Aurnab Ghose

Date: 07-04-2023

Committee:

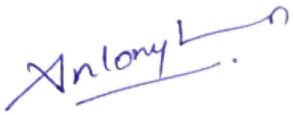
Dr Aurnab Ghose

Dr Nixon Abraham

This thesis is dedicated to my family- for their reckless love.

Declaration

I hereby declare that the matter embodied in the report entitled **Visually guided behaviours in Zebrafish larvae and the role of Fmn2b** are the results of the work carried out by me at the Department of Biology, Indian Institute of Science Education and Research, Pune, under the supervision of **Dr Aurnab Ghose** and the same has not been submitted elsewhere for any other degree



Antony Kiran K David

Date: 01/04/2023

Table of Contents

Certificate 2
Declaration 4
List of Tables 7
List of Figures 7
Abstract 8
Acknowledgements 9
Contributions 11
1 Introduction 12
1.1 Anatomy of Zebrafish visual system 12
1.2 Development of the visual system and behaviour 14
1.3 Visual processing 15
1.4 Circuits in visual behaviour 17
1.4.1 Opto-kinetic Response (OKR) and Opto-motor Response (OMR) 17
1.4.2 Prey-capture 18
1.4.3 Escape responses 19
1.5 Role of Fmn2b 19
1.6 Motivation and objectives 21
2 Materials and Methods 22
2.1 Zebrafish care and maintenance 22
2.2 Free swimming optomotor response 22
2.3 Scoring Scheme for orientation of fish in OMR assay 23
2.4 Restraining larvae for visually guided behaviour assays 24
2.5 Stimulus design and delivery 25
2.5.1 Grating Stimulus for OMR 25
2.5.2 Moving dot for virtual hunting assay 26
2.5.3 Looming circular disc for avoidance assay 26
2.5.4 Grating for OKR 27
2.6 Video Recording 27
2.6.1 High-speed Video Recording for restrained larval experiments 27
2.6.2 Video recording for OMR assay 27
2.7 Data Analysis 27
2.7.1 Automatic tracking for restrained larval experiments 28

2.7.2 Manual tracking for free swimming OMR assay 28
2.7.3 Statistical Analysis 29
3 Results 30
3.1 fmn2b knockout fish shows impaired Orienting response to OMR stimuli ... 30
3.2 StimUNO to perform restrained visually guided behaviour assays 32
3.3 A pipeline for automatic larval tail movement tracking using SLEAP 33
3.4 Automatic analysis of Eye movements using Stytra 35
3.5 Wild-type larvae show avoidance behaviour when stimulated with a looming disc video 36
3.6 Wild-type larvae show saccades when stimulated with whole field moving square gratings 37
3.7 Wild-type larvae elicit hunting manoeuvre when presented with a moving dot 38
4 Discussion 39
5 References 41

List of Tables

Table 1: Summary of various visually guided behaviours..... 15

List of Figures

Figure 1: Structure of zebrafish visual system..... 13
Figure 2: Summary of AFs activity towards different visual cues 17
Figure 3: Hunting Sequence in a free-swimming larval zebrafish..... 18
Figure 4: Schematic showing pathways involved in the hunting response. 19
Figure 5: Effect of FMN2b knockout. 20
Figure 6: Schematic for OMR Assay 23
Figure 7: Scoring function for fish orientation.. 23
Figure 8: Restraining the larvae.. 24
Figure 9: OMR Deficits in fmn2b$^{\Delta 7/\Delta 7}$ zebrafish larvae..... 31
Figure 10: StimUNO for restrained larval experiments. 33
Figure 11: Flowchart for using SLEAP for automatic larval behaviour analysis..... 34
Figure 12: Tail tracking USING a model trained in SLEAP..... 35
Figure 13: Eye tracking by using Stytra..... 36
Figure 14: Sequence of events in a looming disc avoidance assay. 37
Figure 15: Representative tail tracking data from the virtual hunting assay. 38

Abstract

Larval Zebrafish respond to visual stimuli with eye saccades and tail flicks, which depend on the features of the stimuli. Any deficit in these responses indicates a possible defect in visual processing. Studies in the lab have shown that fmn2b$^{\Delta 7/\Delta 7}$ mutant zebrafish larvae have defects in the visual system. We also found deficits in the optomotor response of fmn2b$^{\Delta 7/\Delta 7}$ zebrafish larvae, thus indicating the potential role of Fmn2b in visually guided behaviours. A robust way of stimuli presentation, behaviour recording, and downstream analysis are required to dissect the role of any protein in behaviour. Using an Arduino UNO microcontroller, we designed a platform to perform visually guided behaviour in a partially restrained zebrafish larva, which includes an automatic stimulus presentation unit connected with a high-speed video recording unit- StimUNO. We also developed an automatic pipeline for tracking larval movements, which is flexible and can be adapted to any experimental questions. The reliability of StimUNO and our data analysis pipeline was tested on various behaviours like the looming disc evoked escape response, optokinetic response and virtual prey hunting response. We propose this as a valuable tool in studying the processing of sensory stimuli in larval zebrafish.

Acknowledgements

If I am bright, it is wholly because of the sun that shines upon me[1]. No science can be done in isolation. I am forever grateful to all the brilliant minds who have shaped the world we enjoy today, which enabled me. I thank all the amazing people I am surrounded with, and I promise to spread the kindness and love I received.

I would like to begin by expressing my deepest appreciation to my family, to whom this thesis is dedicated. They have been my support and constants throughout this journey, and I am forever grateful. Thank you Appacha, Ammachi, and Arun!

Before embarking on my thesis, I had the privilege of working with Dr Suhita Nadkarni, an amazing human who has set up one of the coolest labs ever. My experience working in her lab was unforgettable and set the bar really high. It was there that I realized my passion for studying the brain in its complexity. Thank you, Suhita!

I also had the opportunity to represent IISER Pune at the iGEM Competition in 2020, which was my first real research project. It gave me a chance to solve a problem from scratch, and I am thankful to our advisor, Dr Sanjeev Galande, our awesome mentors, Varsha and Tejashree, and the entire team for the amazing experience.

I began my thesis in Aurnab's lab with very little lab exposure right after life started to return to normal after the pandemic. I am grateful to him for trusting me and providing all the help and ideas during my thesis. I thank Roopsali and Saunri for training me in all basic lab techniques. Aurnab's unique mentoring style and discussions were helpful, and I appreciate his patience with me. I also enjoyed the fun during lab meetups and conferences. Thank you, Aurnab!

I would like to thank all the AG lab members, past and present, especially the "fish people," for all the fun moments and discussions.

The Zebrafish facility at IISER Pune played a crucial role in the completion of my thesis, and I express my gratitude to Aishwarya for helping me throughout the final months of my project by maintaining a constant supply of zebrafish embryos.

I feel fortunate to have joined as a BS-MS student, which allowed me to make friends in most labs across departments. Thanks to them, I was always aware of where to look for something when I needed it. Thanks, IISER Pune!

I would also like to thank Vivek from the Science Media Centre at IISER Pune for lending tripods and tips to get good contrast videos for my experiments.

Over the course of my BS-MS life, I have made amazing friends both from IISER and outside, some of whom I have only met online. I am grateful for their support and friendship, which have made my journey more enjoyable. I would like to extend a special note of gratitude to the "Mallu gang" and the "JY family" for providing me with a sense of comfort and belonging throughout my time here.

My thesis would not have been possible without the support of all these wonderful people, and I am forever grateful.

Most importantly, I thank God, who lovingly made sure that I seek beauty, goodness and truth above and beyond another degree.

[1] Adapted from a quote by *C. S. Lewis (1971). "The Four Loves", p.143, Houghton Mifflin Harcourt*

Contributions

Contributor name	Contributor role
AG and AK	Conceptualisation Ideas
AK	Methodology
AK	Software
AK	Validation
AK	Formal analysis
AK	Investigation
AG and AK	Resources
-	Data Curation
AK	Writing - original draft preparation
AG and AK	Writing - review and editing
AK	Visualisation
AG	Supervision
AG	Project administration
AG	Funding acquisition

AG – Dr Aurnab Ghose
AK – Antony Kiran K David

This contributor syntax is based on the Journal of Cell Science CRediT Taxonomy[1].

[1] https://journals.biologists.com/jcs/pages/author-contributions

1 Introduction

Over the course of evolution, vertebrates have developed the ability to perceive their environment through the development of various sensory systems. Of the different senses, such as touch, olfaction, taste, audition, and vision, vision plays a predominant role in sensing the environment in the case of vertebrates like zebrafish. Vision plays a very important role in survival tasks, such as eating and avoiding being eaten. This huge reliance of zebrafish on vision for hunting may be one of the reasons why its visual system develops so fast. A fully developed visual system can be found as early as 5 dpf, which roughly corresponds to the developmental period of exhaustion of yolk supply and the beginning of hunting behaviours (Neuhauss, 2010). The fast external development combined with the transparent nature of the embryos and the amenability of zebrafish larvae to genetic manipulation and whole-brain functional imaging has made it an important model system to probe the development and function of the visual system (Bollmann, 2019; Fleisch and Neuhauss, 2006; Neuhauss, 2010). One of the most significant advantages of studying vision in zebrafish is that functional imaging can be done while the animal responds to complex visual stimuli. Recent advancements have merged genetic, anatomical, and functional data from different experiments into standard atlases (Bollmann, 2019; Kunst et al., 2019; Marquart et al., 2015; Randlett et al., 2015; Ronneberger et al., 2012; Tabor et al., 2019). This has helped in understanding the organisation of the zebrafish visual system, including most of its input, output, and pathways.

1.1 Anatomy of Zebrafish visual system

Zebrafish's visual system has mainly three components: the eye, which receives input from the environment; the visual centres of the brain, which process the information the eye receives; and the neurons that interconnect the eye to the visual centres of the brain, called the retinofugal projections (Fleisch and Neuhauss, 2006; Neuhauss, 2010). At 5 dpf, the larval retina contains all the typical layering seen in other vertebrates (Branchek, 1984; Fleisch and Neuhauss, 2006; Neuhauss, 2010). The retina of the zebrafish contains photoreceptors, rods, and cones. Unlike humans, who have three types of cones, zebrafish have four, making them tetrachromatic. The extra type of cones also makes them sensitive to light in the UV

spectrum (Cameron, 2002; Robinson et al., 1993). This might be an adaptation for prey tracking in the water since UV light, being shorter wavelength, scatters more easily in water. So if an object emits UV, it should be nearby, which helps track nearby prey (Yoshimatsu et al., 2020). Some reports show that even though rods and cones are detectable from 5 dpf, the contribution of rods is negligible, making the larval retina a functionally cone-dominated one (Bilotta et al., 2001).

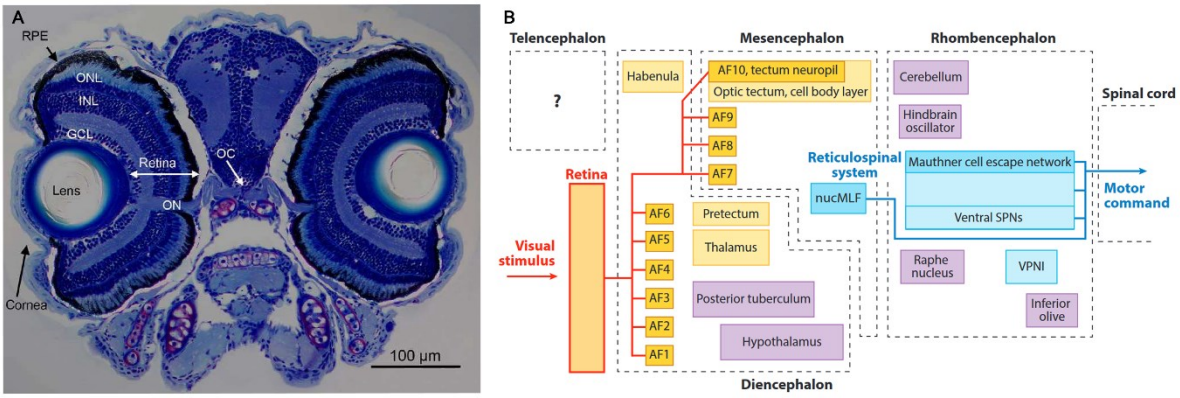


Figure 1: ***Structure of zebrafish visual system****. A) A histological section through a 6 dpf larva (Neuhauss, 2010). B) Schematic representation of different connections in the larval visual system (Reproduced from Bollmann, 2019).*

Figure 1.A shows the histological section through the eye of a 6-day-old zebrafish larva. The Retinal pigmented epithelium (RPE) nourishes the photoreceptors and supports them. The outer nuclear layer (ONL) hosts the photoreceptors, while the inner nuclear layer (INL) has the cell bodies of other neuronal cell types in the retina as well as glial cells. The Ganglion cell layer (GCL) contains cells that form long axons comprising the optic nerve (ON) and optic tracts. Apart from these, the anterior parts of the eye contain the lens and cornea to refract light rays and help to focus them onto the retina (Fleisch and Neuhauss, 2006; Neuhauss, 2010).

The parts of the brain that are active when visually stimulated are primarily the optic tectum, the pretectal areas, and the thalamus, which are sensitive to specific visual stimulus features. Once the brain processes the visual information and commits to performing one of the many possible actions, the motor commands are relayed from the brain to the spinal cord through the reticulospinal (RS) neurons in the nucleus of the medial longitudinal fasciculus (nucMLF) in the hindbrain, which activates the motor neurons either directly or indirectly through interneurons. Apart from these areas, regions like the cerebellum and some structures in the rhombencephalon and

diencephalon are active during visually guided behaviours. These have functions yet to be explored completely, but some may represent internal states or motor learning, among others (Bollmann, 2019). These connections are summarised in the schematic shown in Figure 1B.

The retinofugal projections are the neural pathway that leaves the eyes and ends in the optic areas of the brain. In the case of fish, it is the Optic tectum and its associated arborisation fields. This is also an important system for studying axonal guidance and pathfinding. Unlike humans, which have both ipsilateral and contralateral projections, it is only contralateral in zebrafish and forms a complete optic chiasma (OC). The projections to the optic tectum have an inverted topographic map arrangement to represent the external environment. Apart from the tectum, these also project to nine other arborisation fields (AFs) (Baier and Wullimann, 2021; Bollmann, 2019; Fleisch and Neuhauss, 2006; Neuhauss, 2010).

1.2 Development of the visual system and behaviour

The visual system starts its development with the eye developing around 10 hpf (hours post-fertilisation). The ganglion cells of the GCL layer differentiate at about 32 hpf, with their axons starting to project to the optic tectum. By 55 hpf, rods and cones can be detected and form synaptic terminals. By 70 hp, functional ribbon synapses arise in photoreceptor terminals and bipolar cell synapses. This marks the time at which the larvae elicit their first behaviour in response to light - the startle response, where the larvae respond to sudden increases in illumination by rapidly turning away from their source. At 3 dpf, the retinal layers are differentiated, and synapses are formed. At this point, the larvae can respond to Optic flow and show optokinetic responses (OKR). OKR tracks the movement of the eye in response to optic flow. When a whole field grating stimulates the larvae, it responds by saccadic eye movement. Older larvae post 6 dpf tend to move in the direction of moving square grating. This behaviour is called optomotor response (OMR). Post 6dpf larvae, having a fully functional visual system, can also exhibit both hunting and predator avoidance behaviour (Bollmann, 2019; Fleisch and Neuhauss, 2006; Neuhauss, 2010). Table 1 summarises the common visually guided behaviours discussed here and the days on which they can be elicited robustly and is not an exhaustive list.

Behaviour	Response	Time point
Startle response	When there is a sudden change in illumination, the larvae turn away from the source.	3 dpf
Opto-Kinetic Response (OKR)	Larvae track the stripes and show saccadic eye movements when shown a whole field moving square grating.	3 dpf
Opto-motor Response (OMR)	Larvae align themselves and move in the direction of the moving square grating below.	6 dpf
Prey hunting	A prey-like stimulus can start the characteristic prey capture manoeuvres	6 dpf
Predator avoidance	When stimulated with a predator-like object, the larvae show a typical C-bend and try to swim away from the direction of its approach.	6 dpf

Table 1: ***Summary of various visually guided behaviours*** *(Fleisch and Neuhauss, 2006; Neuhauss, 2010).*

The development and proper functioning of the zebrafish visual system are highly dependent on various internal and external factors. Evidence suggests that constant light or dark conditions during larval development will lead to deficits in visual behaviour, including decreased spectral sensitivity. So, the light-dark cycle is critical in larval rearing for the proper development of the visual system. Studies have verified this using visual behaviour assays and electroretinography (ERG). Studies have also shown the increased threshold for light intensity for adult escape response, suggesting decreased sensitivity to light during night-time. This points to the importance of considering the time of the day for conducting any visually guided behaviour assays (Fleisch and Neuhauss, 2006; Neuhauss, 2010).

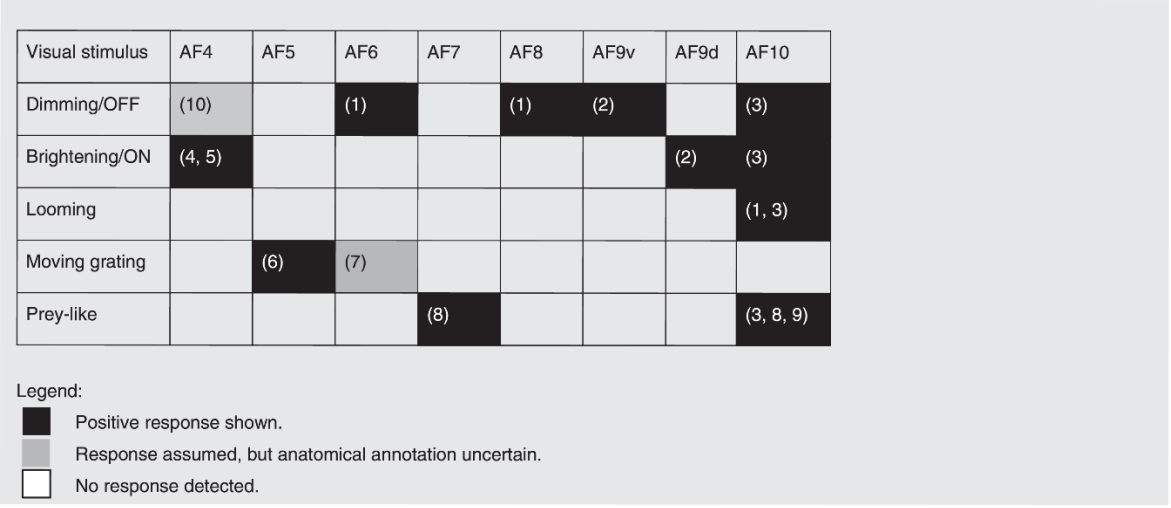
1.3 Visual processing

The photoreceptors undergo graded hyperpolarisation in response to light, which ultimately causes the Retinal ganglion cells (RGCs) to fire action potentials. This graded potential of the photoreceptors becomes spiking activity at the axon terminals

of bipolar cells. Across the entire population of these terminals, the luminance change of the light can be encoded. Bipolar cells are also responsible for chromatic responses in the larval retina because of their diverse spectral responses (Baden et al., 2011; Dreosti et al., 2011; Zimmermann et al., 2018).

The retina contains RGCs tuned to the stimulus's orientation and direction, leading to orientation and direction elective signals. Some RGCs are tuned for size selectivity with a preference for small visual stimuli with an angular size corresponding to the size of their prey. Thus, visual features like size, direction, and orientation are processed in the retina. These features are then fed in parallel into multiple visual areas with different processing roles (Bollmann, 2019; Preuss et al., 2014; Semmelhack et al., 2014).

As described earlier, the retinofugal connection projections project to 10 arborisation fields (AFs), of which the 10th and most prominent one is the Optic tectum. The AFs are numbered based on their position in the optic tract. For the table, the AF identities follow the system described in Baier and Wulimann, 2021. It is thought that different AFs are involved in processing a particular feature of visual stimuli. This has been verified in recent studies coupling behaviour with calcium imaging, ablation, and optogenetic manipulations. The available literature has been summarised by Baier and Wullimann, 2021, and is shown in Figure 2. For example, AF7 is highly selective for small objects and is active when a prey-like stimulus is shown (Baier and Wullimann, 2021; Bollmann, 2019; Semmelhack et al., 2014).



Notes: References: (1) Temizer et al. (2015), (2) Robles et al. (2014), (3) Förster et al. (2020), (4) Zhang et al. (2017), (5) Lin and Jesuthasan (2017), (6) Kramer et al. (2019), (7) Naumann et al. (2016), (8) Semmelhack et al. (2014), (9) Bianco and Engert (2015), (10) Heap et al. (2018).

*Figure 2**: **Summary of AFs activity towards different visual cues** (Reproduced from Baier and Wullimann, 2021).*

With this information in hand, dissecting defective circuits in the case of a mutant larva is now more convenient. The table also shows that the optic tectum is involved in almost all visually guided behaviours described except for moving grating. This means that OMR and OKR cannot pick up defects in the tectum, as shown through ablation studies. Similarly, extensive behavioural analysis can, in turn, help to identify possible defective circuits in the visual system.

As a result of proper axonal guidance and pathfinding, the temporonasal and dorsoventral axes of the retina are mapped onto the rostrocaudal and lateromedial axis of the tectum, respectively. So, any defect in axonal pathfinding may reflect on the topography. This preliminary map formed during development will be refined by experience (Bollmann, 2019).

1.4 Circuits in visual behaviour

1.4.1 Opto-kinetic Response (OKR) and Opto-motor Response (OMR)

Here the fish moves the eyes in a saccadic motion in response to whole-field motion mimicked by moving square grating. A schematic of information flow during OKR is shown in the Figure.

The whole-field motion is detected by the RGC and is transmitted to the pretectal areas. For OKR, the pretectum directly or indirectly activates the oculomotor system

to control the extraocular muscles. In the case of OMR, the swimming is activated by the nucMLF and the RS system, which receives projections from the pretectum. The nucMLF and RS neurons extend their axons to the spinal cord to directly control swimming (Bollmann, 2019; Kramer et al., 2019; Kubo et al., 2014).

1.4.2 Prey-capture

5 dpf larvae can feed by tracking and hunting small prey. Once a prey enters the visual field, the eyes converge to get the prey in a binocular visual field and are maintained until the behaviour is over, which lasts for around 1-2 seconds. The larva elicits a typical J-turn to orient itself to the prey's direction and is concluded by a capture swim and strike, leading to the prey's engulfing. The typical J-turn is elicited by object sizes less than 5^0 both in free swimming as well as in restrained larvae (Bianco et al., 2011; Bollmann, 2019; Fleisch and Neuhauss, 2006; Neuhauss, 2010; Semmelhack et al., 2014). The sequence of events is shown in Figure 3.

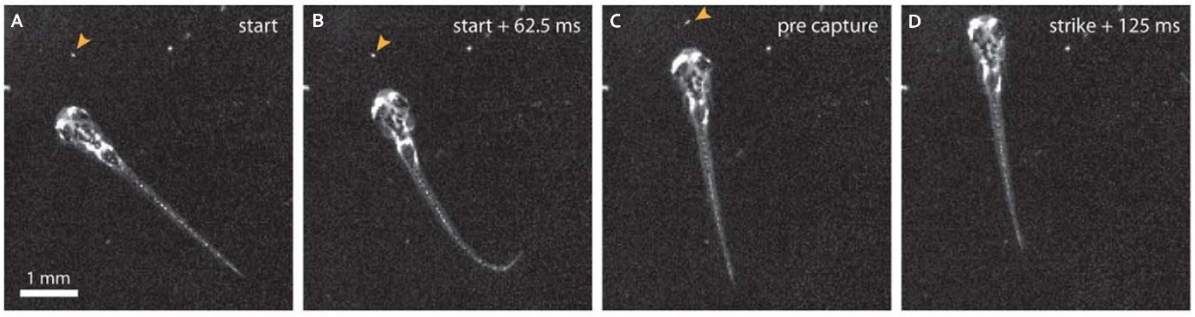


Figure 3: ***Hunting Sequence in a free-swimming larval zebrafish****. A) Prey (marked with orange arrowhead) in the visual field of the larva. B) J-turn to orient towards the prey. C) Larva just before capture D) Prey is engulfed. (Reproduced from Bianco et al., 2011)*

RGC cells tuned to the stimulus corresponding to prey size project to tectum and AF7. These two are 2 possible parallel processing pathways for prey-related stimuli. The tectum likely relays the signal to the hindbrain, which encodes the amplitude of the turn. The role of the pretectal pathway is not fully known but is thought to gate the swim event. Figure 3 summarises these connections, but how these pathways interact is not fully understood. Studies have also shown a component in the pretectal pathway with projections to the feeding centre of the hypothalamus, which may play a motivational role (Bollmann, 2019).

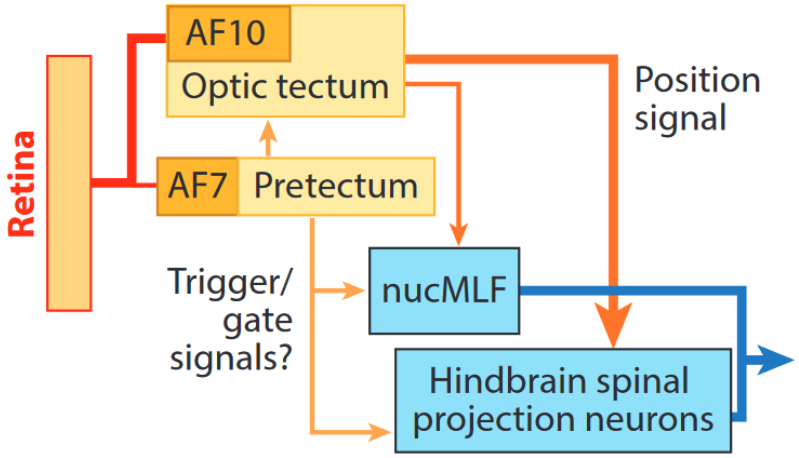


*Figure 4: **Schematic showing pathways involved in the hunting response**. (Reproduced from Bollmann, 2019)*

1.4.3 Escape responses

The predator avoidance behaviour can be elicited in the laboratory by showing a looming disk to free-swimming or restrained larvae. The final angular size of the disk and its expansion rate determines the robustness of the response. Once the larva encounters the disk, the immediate response is C-bend, which turns it away from the object, followed by a fast-forward swim to propel itself away from the stimulus (Bollmann, 2019; Fleisch and Neuhauss, 2006; Neuhauss, 2010; Temizer et al., 2015).

The processing of the looming stimuli occurs mainly in the deeper layers of the tectum. The looming rate affects the kind of response; the faster rates trigger stereotypical escapes, while slower looming triggers more variable escape paths. There have been reports of an indirect pathway with projections from the tectum to the thalamus, which can modulate looming response (Bollmann, 2019). The pathways underlying the looming escape response are still under investigation but can be primarily considered as a reflex.

1.5 Role of Fmn2b

Fmn2b belongs to a family of proteins known as formin, which are involved in cytoskeletal remodelling. They are actin nucleators and are characterised by the FH1 and FH2 domains. Formin-2, or Fmn2, is found to be enriched in the developing and mature nervous systems of many organisms and has been indicated in

neurodevelopmental disorders, intellectual disability, age-related dementia, microcephaly, and sensory processing dysfunction in humans (Agís-Balboa et al., 2017; Almuqbil et al., 2013; Anazi et al., 2017; Law et al., 2014; Marco et al., 2018; Nagar et al., 2021b; b).

In zebrafish, the fmn2 gene has 2 isoforms: fmn2a and fmn2b. Studies in the lab have reported that fmn2b is enriched in the RGCs in the developing zebrafish embryo and that its knockout leads to defects in several pathways, including the visual system. Some of the defects seen in the visual system are the thinning of the optic nerve, reduction in the RGC arborisation in the optic tectum, and deficits in the inter-tectal neuron (Nagar, 2021).

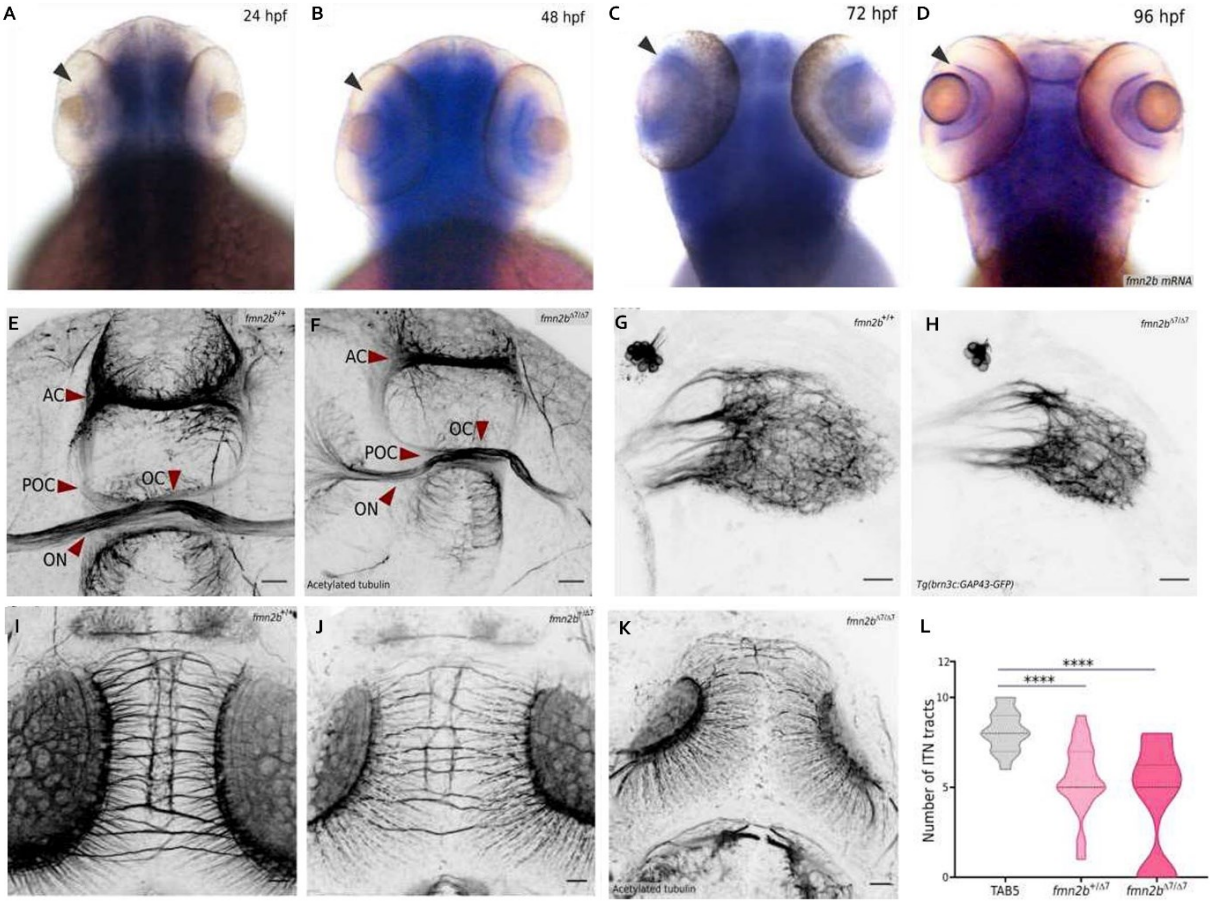


Figure 5: ***Effect of fmn2b knockout on larval zebrafish****. A-D) fmn2b mRNA localisation across different developmental stages. E-F) Effect of fmn2b on optic nerve thickness. E is wild-type, and F is mutant. G-H) Effect of fmn2b on tectal arborisation. G is wild-type, and H is mutant. I-K) Effect of fmn2b on inter tectal neurons. I is wild type, H is heterozygous mutant and K is homozygous mutant. L) Quantification of inter tectal neuron numbers. (Reproduced from Nagar, 2021)*

1.6 Motivation and objectives

Zebrafish is an excellent model system to study vertebrate visual systems. One main advantage of using this model is the ability to do extensive behavioural analysis to dissect the role of a gene in behaviour and its genetic amenability (Nagar et al., 2021a). Most of the behavioural responses of the zebrafish involve eye saccades and tail flicks, which happen on a very fast time scale, and high-speed recording is needed to study such behaviours. Earlier experiments in the lab involving fmn2b$^{\Delta 7/\Delta 7}$ zebrafish larvae have shown defects in their visual system (Nagar, 2021). This motivated us to check for deficits in visually guided behaviours, such as the optomotor response (OMR) in fmn2b$^{\Delta 7/\Delta 7}$ larvae. Since a more extensive behavioural analysis has to be done to dissect the role of Fmn2b in behaviour, we wanted to develop a platform that can reliably record videos at high-speed and present different visual stimuli automatically with minimum human intervention.

Manual scoring will introduce biases and limit data reproducibility if we record larval movements at high speed. To solve this problem, we wanted to develop an automatic larval movement tracking pipeline. Since different experiments call for different kinds of analysis, we wanted our analysis pipeline to be flexible and adaptable to the requirements of the experiment.

Developing such a platform and analysis pipeline will significantly contribute to performing extensive behaviour analysis and help researchers study how the zebrafish process sensory stimuli.

Objectives

- To characterise the defects in the optomotor response of the fmn2b$^{\Delta 7/\Delta 7}$ larvae
- To design a system to perform visually guided assays for zebrafish larvae which is capable of high-speed video recording and automatic stimulus delivery.
- To develop an automatic pipeline to analyse the larval movements, which can be easily adapted to the experimental questions.

2 Materials and Methods

2.1 Zebrafish care and maintenance

Wild-type strains of zebrafish (TAB5) bred in the facility and in-crossed for at least one generation were used for all the experiments in this study. Adult zebrafish were raised in a continuous water-recirculating aquarium system (Techniplast) at 28^0C and 7.4 pH under a 14/10-hour light-dark cycle. Embryos were collected by natural breeding and were raised in E3 medium (5 mM NaCl, 0.33 mM MgSO4, 0.17 mM KCl, 0.33 mM CaCl2, and 10^{-5} % methylene blue) ("E3 Medium (for Zebrafish Embryos)," 2011) at 28°C and used at 5dpf for the experiments. Adult fish was fed three times daily with a mix of live artemia and dry powder feed (Zeigler).

The mutant strain used in this study, fmn2b$^{\Delta 7/\Delta 7}$, was generated in the lab and was maintained in the same conditions are in the wild-type fish.

The larvae were raised in 10 cm Petri plates with E3 medium changed regularly, and dead embryos and other debris were also removed. For experiments that needed 6 dpf or older larvae, at the end of 5 dpf, they are fed larval feed in the Petri dish itself and repeated until needed.

2.2 Free swimming optomotor response

Zebrafish Larvae are raised till 7 dpf as described. On the seventh day, 10 larvae are placed on a 10 cm square Petri dish filled with 50 mL of E3 without methylene blue at 28^0C on top of an LCD monitor (Lenovo L151), as shown in Figure 6. The larvae are allowed to acclimatise to the setup for 5 minutes at room temperature. The LCD screen will be projecting a blank white screen during this period. A square grating is generated using custom codes using PsychoPy (Peirce et al., 2019) in Python and is projected on the entire screen in full-screen mode. The sides of the Petri dish are lined with masking tapes such that the larvae cannot see anything beyond the plate. The square grating had a width of approximately 114.6^0 and moved at a speed of 5.4^0/s.

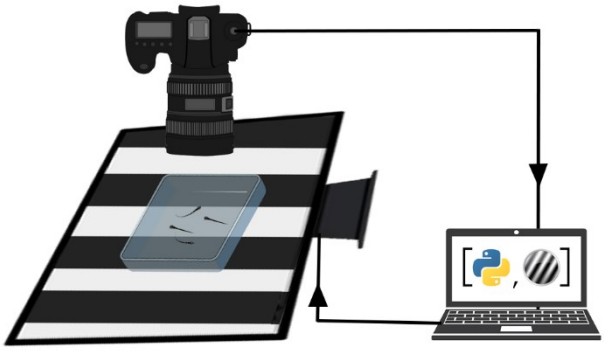


Figure 6: ***Schematic for OMR Assay***

2.3 Scoring Scheme for orientation of fish in OMR assay

The coring scheme was such that the larvae oriented towards the direction of the stimulus got a score of 1 (90^0), and the one oriented opposite got a score of -1 (-90^0). The larvae that are oriented perpendicular get a score of 0 (0^0, -180^0, 180^0), and the remaining orientations get a score which can be described by a linear function.

The scoring function can be described as shown in Figure 7.

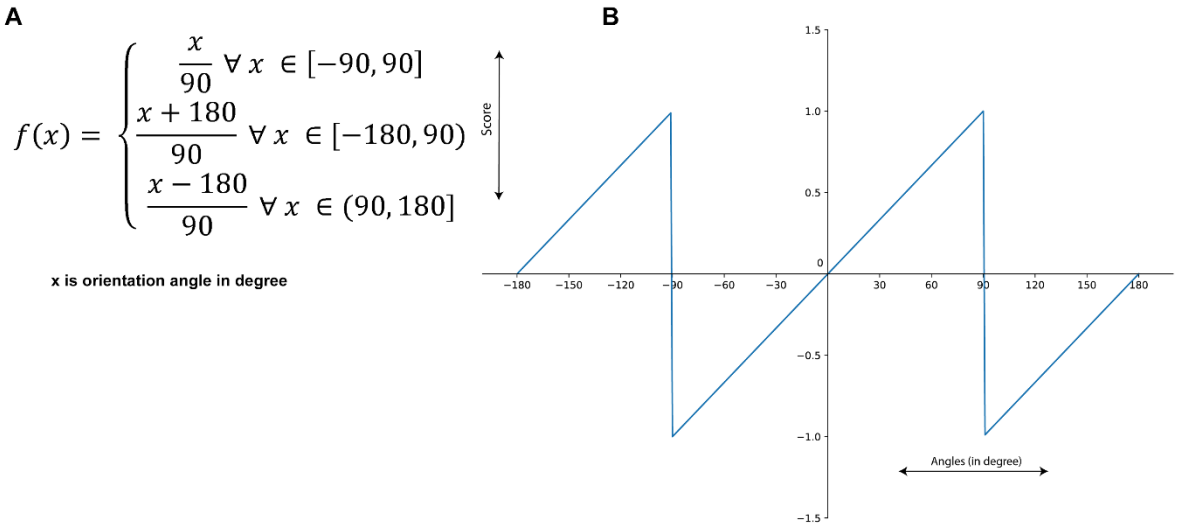


Figure 7: ***Scoring function for fish orientation****. A) The function describing the scoring scheme. B) The scores are plotted against all possible orientations.*

Snapshots were taken just before and after stimulus delivery, and the mean orientation angle was calculated using the above scheme in a custom python code.

2.4 Restraining larvae for visually guided behaviour assays

The larvae were raised as described. At 5 or 6 dpf, the larvae were anaesthetised in 0.02% tricaine (MS-222, Sigma) (Leyden et al., 2022) and were restrained in 2% low melting point agarose (Sigma). 0.02 % (~168 mg/L). A 2.5x stock was prepared by dissolving 50 mg of tricaine (M-222, Sigma) in 100 mL of 1X E3 solution ("E3 Medium (for Zebrafish Embryos)," 2011), and the pH was adjusted to 7 using 1 M Tris (pH 9) and was stored in 4^0 with the container wrapped in aluminium foil. A few hours before use, 10 mL of 1x tricaine was made from the 2.5x stock and was kept in a 28^0 incubator.

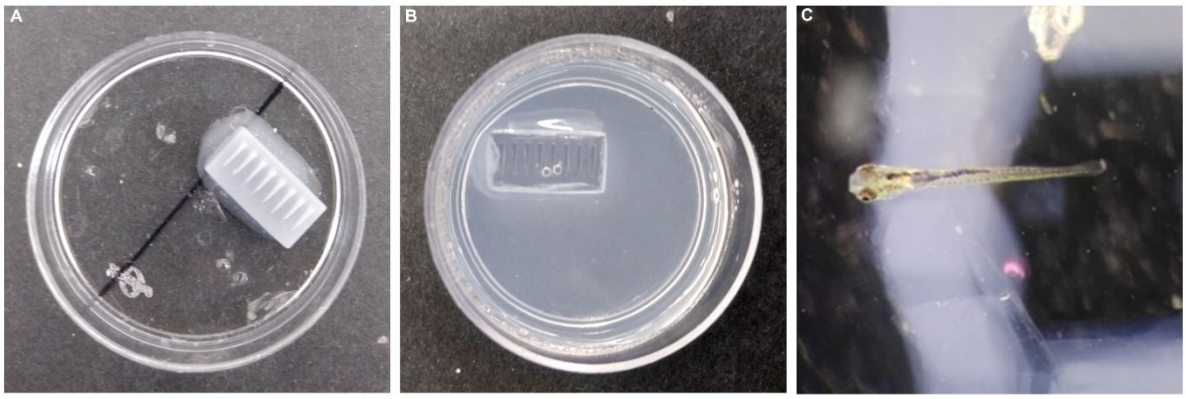


Figure 8: ***Restraining the larvae****. A) The 3D-printed comb attached to the lid of a 3.5 mm Petri plate. B)1% agarose bed made on a 3.5 mm Petri plate. C) A partially restrained larvae that can move both its eyes and tail.*

To ensure that the larvae stay in almost the same depth and position across different trials, a specific way of mounting was used, adapted from a previous study (Geng and Peterson, 2021). A comb, as described in Geng & Peterson, 2021 was 3D printed and was pasted onto the lid of a 3.5 cm Petri dish approximately 1 cm from the edge and the last ridge on the comb aligning with the diameter of the lid as shown in Figure 8A**.** It was secured in place using silicon-based glue. As shown in Figure 8B, this comb attached to the lid will be used to make a 1% agarose bed on a 3.5 cm Petri plate. To restrain the larvae, 2% low melting agarose (Sigma) is made and kept in a 37^0 incubator until use. On the evening before the planned experiments, 10-20 larvae are transferred to 0.002% tricaine solution in E3 medium at 28^0C and are incubated for no more than 10 minutes. Using a dropper, a drop of low melting point agarose is transferred to a clean Petri plate, and one anaesthetised larva is kept on it using a clean pointed paintbrush. The larva, along with the gel, is transferred carefully using a dropper onto the previously made bed and is then filled

with more low melting point agarose till it forms a layer over the bed. Once the low-melting-point agarose is set, it is topped with E3 medium without methylene blue to prevent drying. The gel around the tail and the eyes is carefully removed using surgical forceps and scalpels. After this, the larvae can freely move its tail and eyes, as shown in Figure 8C. 3- 4 restrained larvae are then kept in a 10 cm Petri plate with little Milli-Q water, covered, and kept in the larval incubator at 28^0C overnight for habituation. The Milli-Q water ensures the gel does not dry off and the larvae stay moist. Approximately 1 hour after the light turns on the following day, they are used for further behavioural assays.

2.5 Stimulus design and delivery

Custom python scripts were made on top of PsychoPy (https://www.psychopy.org/) to generate and deliver the stimulus. The stimuli consisted of a small moving dot, static square grating, moving square grating and a looming dot. The python scripts can be found at https://github.com/antonykiran10/StimUNO. The stimulus's parameters are specified in terms of pixels in the code and converted into visual angles based on a calibration of the display used. All the stimuli were in black and white and with maximum contrast. The stimuli were delivered keeping the ambient light turned on and were illuminated from below using a custom-made IR LED array with peak emission at 850 nm. The larvae were acclimatised for 5 minutes by projecting a white screen while keeping the IR on so the fish gets used to the experimental conditions. For the restrained larval experiments, the projector was fixed at a distance of 8.5 cm from the screen, with the focus slider set to the minimum.

2.5.1 Grating Stimulus for OMR

A square grating was used to elicit OMR. The grating was projected in full-screen mode, and each grating had a width of 1 cm. The spatial frequency of the grating was set to be 2 cycles per 230 pixels. Since the maximum water level in the Petri plate was 0.5 cm, this was assumed to be the distance of the larvae from the screen and was used in computing visual angles. Assuming the above holds, each grating subtended a visual angle of 114.6^0.

The monitor had a refresh rate of 60 Hz (Lenovo L151 monitor). This implied that each frame is displayed for a period of 1/60 s which is approximately 16.7 ms. Since

Psychopy projects each frame with respect to the monitor's frame rate, the phase of the moving grating could be calculated based on this. The code was written such that the grating moves 0.05 px per frame, which gives us a frame rate of 3 px/s. Based on the previous calibration of grating size, this can be converted into visual angles and is 5.4^0/s. The parameters were finalised based on trial and error.

2.5.2 Moving dot for virtual hunting assay

A small black dot moving from one end of the screen to the other at a constant speed was used to elicit the hunting behaviour. The initial position of the dot used in the python script is set based on trial and error such that it moves at the height of roughly 0.5 cm from the bottom of the 3.5 mm Petri plate used and sweeps an angle of more than 120^0 from one end to the other. The groves for the larvae made by the comb align fish at 0.5 cm from the bottom and 1.1 cm from the end. So, the distance of the larvae from the screen was taken to be 1.1 cm for calculating the visual angle. The dot diameter projected onto the screen was 0.1 cm, giving us a visual angle of 5.2^0. Since the projector (Sony MP-CD1) projected at a frame rate of 60 Hz, each frame was projected for 16.7 ms as earlier. The code was written such that the dot moves at a speed of 4 px per frame, which gives us a speed of 90.2^0/s. These stimulus parameters were adapted from Bianco et al. 2011 (Bianco et al., 2011).

2.5.3 Looming circular disc for avoidance assay

A looming dark disc which starts as a small dot and then expands till it covers the entire white screen circularly, was projected directly in front of the larvae to elicit the avoidance behaviour. The dot's position was specified in the code from trial and error such that it is directly in front of the larvae and at the height of 0.5 cm. Distance of the larvae from the screen was the same as in the case of the virtual hunting assay, ie. 1.1 cm. The initial size of the dot was approximately 0.1 cm which subtends a visual angle of 5.2^0. The radius of the dot is set to increase at a speed of 2.2 px per frame. Moreover, since the projector has a frame rate of 60 Hz, each frame is presented for 16.7 ms. Apart from this, an additional delay of 10 ms is set in the code to control the speed. Both the delays together, each frame is projected for 26.7 ms. This sets the rate of increase of the radius to be 82.4 px/s which is roughly 31^0/s. These stimulus parameters were adapted from Temizer et al. 2015 (Temizer et al., 2015).

2.5.4 Grating for OKR

For OKR, the grating was projected on the walls of the Petri plate as in both virtual hunting and looming evoked escape response. The larva had a distance of 1.1 cm from the screen. The grating was projected in full-screen mode, with each grating having a width of 21.7^0 and a spatial frequency set the same as that used in the OMR stimulus. The speed of the moving grating was set to be 0.05 px per frame which corresponds to a speed of 1.13^0/s. The parameters were finalised based on trial and error.

2.6 Video Recording

2.6.1 High-speed Video Recording for restrained larval experiments

A camera capable of high-speed recording (AVT Pike F032B ASG) fixed with an AZURE-3514MM lens and 850 nm bp filter (Azure Photonics) and an IR LED array for illumination. The camera was controlled using the manufacturer's software (AVT Fire Package) running on a PC running Windows 7 Professional (Intel i7-4770 CPU @ 3.40 GHz, 16 GB RAM) with additional hardware interfaces from the manufacturer. For recording at 120 fps for 60 s, a frame buffer of 5000 was set. The trigger mode was left at default.

2.6.2 Video recording for OMR assay

A Canon EOS 1500 D DSLR was used to record videos of the OMR assay. The recording mode was set to monochrome. The camera was controlled using the proprietary software EOS Webcam Utility on a PC running Windows 11 Home Edition (AMD Ryzen 5 3550H @ 2.10 GHz, 8 GB RAM) connected via a USB cable.

2.7 Data Analysis

Unless explicitly mentioned otherwise, all the analysis and SLEAP training have been done on a Workstation running Ubuntu 22.04 (Intel Xeon® E-2278G CPU @ 3.4 GHz x16, 64 GB RAM, NVIDIA Quadro P2000).

All the custom codes used are available on this repository: https://github.com/antonykiran10/StimUNO

2.7.1 Automatic tracking for restrained larval experiments

Since the status of stimulus delivery is marked in each frame using the SIS feature of the camera, the first step is getting that information. The SIS was encoded in binary in row 3 of the captured image, and the 32nd bit in that row contained information regarding the stimulus status. The camera input pin 1, which was colour-coded grey, was used to send TTL pulses to the camera using n HR10A-10P-12S connector for this project. A custom python code was written on top of MeenKando (https://gitlab.com/tomin-james/meenkando) to extract that and annotate each frame with time stamp and stimulus status in human-readable form and also to save that information as a CSV file for further analysis.

The raw data from SLEAP is stored as an HDF5 file. During tracking, it is possible that in a few frames, the tail tip was so faded that it could not be tracked. To avoid these missing coordinates hindering further analysis, we filled it up using the value from the adjacent frame just before. This correction did not impart many discrepancies in the data since the rate was found to be very low. A way to check if this error is building up is by looking at the coordinate over the frame and seeing if there is plateauing happening away from the rest position of the tail, which should be interpreted as the model is inadequate and needs to be trained further. A way to look at the tail position is to calculate the tail tip angle by dividing the y-coordinate with the x-coordinate and correcting it with the rest position, which is implemented by custom python codes. The eye angles are determined using Stytra (Štih et al., 2019) and stored as a CSV file.

All this raw data can be used for different kinds of analysis depending on what parameter we need to consider.

2.7.2 Manual tracking for free swimming OMR assay

The video was recorded at 30 fps. For the purpose of analysis, we will be looking at 2 fps. The fish's position at each frame was tracked using the manual tracking plugin in Fiji (Schindelin et al., 2012), and the coordinates was saved as a TSV file. The file was imported to the ibidi chemotaxis and migration tool (Chemotaxis and Migration Tool | Free Software) to extract the distance, displacement and velocity.

To determine each larva's orientation angle in the snapshots before and after stimulus delivery, we used the arrow ROI marker tool in Fiji (Schindelin et al., 2012)

to mark those larvae and measured the angle of the direction of the arrowhead and saved them as a CSV file. This raw data was analysed using custom python codes after required preprocessing.

2.7.3 Statistical Analysis

All statistical analysis was done using the SciPy (Virtanen et al., 2020) module using custom scripts. The Mann- Whitney U test was used to check the statistical significance of mutant and wild-type data.

3 Results

3.1 fmn2b knockout fish shows impaired Orienting response to OMR stimuli

Optomotor response (OMR) is a very robust response shown by Wild type larvae from 6 dpf onwards (Fleisch and Neuhauss, 2006), in which the larvae orient themselves and move in the direction of a moving square wave grating. In order to check the response of fmn2b$^{\Delta 7/\Delta 7}$ zebrafish for deficits in optomotor response (OMR), we designed the following assay. Zebrafish larvae were raised to 7 dpf following standard protocols (see Materials and Methods). On the day of recording, 10 larvae were transferred to a square Petri plate filled with 1x E3 medium. The Petri plate was kept on a computer monitor laid flat, and moving square grating of width 114.6^0 and phase of 5.4^0/s was displayed. A camera was placed on top to record the behaviour. We found that wild-type zebrafish orients itself in the direction of the grating and swims in its direction. The orientation of the larvae before and after stimulus presentation was found and scored such that the fish oriented towards the direction of grating gets maximum value, and the one opposite gets minimum value (see Materials and Methods). Also, the fraction of fish present in the plate's half in the direction of the grating is determined. These measurements are used as an indication of the larva's optomotor response, and a deficit in this may suggest a defect in the neural pathways involved in this behaviour.

Our data suggested a deficit in the OMR response of fmn2b$^{\Delta 7/\Delta 7}$ larvae, as it failed to orient in the direction of the moving grating (Figure 9.A, Figure 9.G-H). However, there was no difference in the fraction of larvae that moved in the direction of the grating between wild-type and fmn2b$^{\Delta 7/\Delta 7}$. (Figure 9.B-C). This indicated that though fmn2b$^{\Delta 7/\Delta 7}$ larvae have a problem orienting in the direction of the stimulus, they could swim in its direction.

Since the fraction of larvae crossing half and 5/6th of the plate in the direction of the grating is not different (p-value = 0.5 and 0.08 respectively) for wild-type and fmn2b$^{\Delta 7/\Delta 7}$ (Figure 9.B-C), we evaluated the distance travelled by the larvae along with its displacement and velocity. Since automatic tracking was difficult due to the moving grating in the background, we manually tracked the larval movements (see Materials and Methods). Data suggested that fmn2b$^{\Delta 7/\Delta 7}$ mutant larvae may be following a long path as it tries to move in the direction of the stimulus (Figure 9.E-F, I-J). The mean distance travelled by the fmn2b$^{\Delta 7/\Delta 7}$ larvae is 80.63 ± 4.76 mm (Mean + Std. dev.), and that by wild type is 58.98 ± 8.4 mm (Mean + Std. dev.) (p-value < 0.0001). There was no difference between the displacement of fmn2b$^{\Delta 7/\Delta 7}$ and wild-type larvae (p-value = 0.2786). There was also an increase in the velocity of the fmn2b$^{\Delta 7/\Delta 7}$ larvae (p-value < 0.0001).

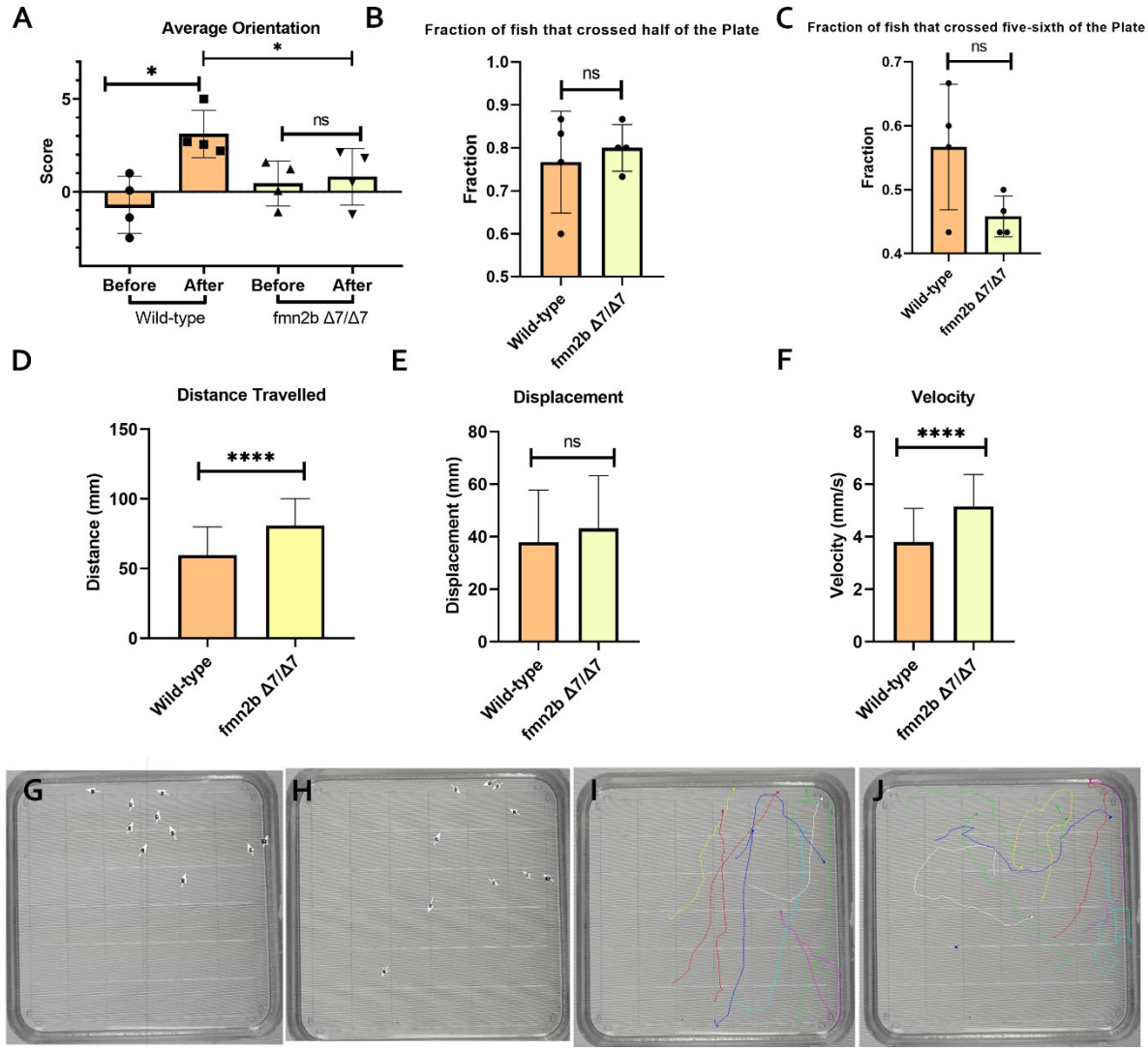


Figure 9: ***OMR Deficits in fmn2b$^{\Delta7/\Delta7}$ zebrafish larvae****. **A-C)** Average values for wild-type and fmn2b$^{\Delta7/\Delta7}$ larvae are plotted for 4 sets of experiments. Each experiment set consists of 3 trials with 10 larvae, and the average of 3 trials is plotted for each set. The before and after labels indicate the average score before and after stimulus presentation, respectively. A) Mean orientation scores of larvae (see Materials and Methods). The average of scores before and after stimulus delivery for wild-type is different (p-value = 0.0286), while that of fmn2b$^{\Delta7/\Delta7}$ is not (p-value = 0.6857). Average scores post-stimulus presentation for wild-type and fmn2b$^{\Delta7/\Delta7}$ are also different (p-value = 0.0286). B) Mean fraction of fish in the half that is in the direction of the moving square wave grating. The average fraction of fish in the half of that plate in the direction of the moving grating is not different in the case of wild-type and fmn2b$^{\Delta7/\Delta7}$ (p-value = 0.9714). C) Mean fraction of fish that crossed 5/6th of the plate in the direction of the moving square grating. The average fraction of fish that crossed 5/6th of the plate in the direction of the moving square grating is not different in the case of wild-type and fmn2b$^{\Delta7/\Delta7}$ (p-value = 0.2). **D-F)** Individual values of distance travelled, displacement and velocity for wild-type and fmn2b$^{\Delta7/\Delta7}$ larvae are plotted for 29 larvae across 4 sets of experiments for both wild-type and fmn2b$^{\Delta7/\Delta7}$. Each experiment set consisted of 1 trial with 9-10 larvae, and the individual values for each larva are plotted. D) Distance travelled by the wild-type and fmn2b$^{\Delta7/\Delta7}$ larvae are different (p-value <0.0001). E) Displacement of the wild-type and fmn2b$^{\Delta7/\Delta7}$ larvae are not different (p-value = 0.2786). F) Velocity of the wild-type and fmn2b$^{\Delta7/\Delta7}$ larvae is different (p-value < 0.0001). **G-J)** Photograph of larvae during OMR assay for a single trial. The arrows in G and H are marked using Fiji (see Materials and Methods), where the arrowhead indicates the position of the head of the larvae. The lines in different colours mark the path followed by each larva during the 15s OMR stimulus presentation. Each colour represents the path of one individual larva (see Materials and Methods). G) Photograph with the orientation of wild-type larvae after stimulus presentation. H) Photograph with the orientation of fmn2b$^{\Delta7/\Delta7}$ larvae after stimulus presentation. I) Path followed during OMR by wild-type larvae. J) Path followed during OMR by fmn2b$^{(\Delta7/\Delta7}$ larvae.*

*For A-F, * indicates a statistical significance (p-value < 0.05), ** indicates a statistical significance (p-value < 0.01), *** indicates a statistical significance (p-value < 0.001), **** indicates a statistical significance (p-value < 0.0001) and ns indicates that the difference is not statistically significant (p-value> 0.05). P-value was determined using the Mann–Whitney U test.*

3.2 StimUNO to perform restrained visually guided behaviour assays

Since the OMR assay suggested that FMN2b is involved in the development and function of the OMR pathway, we wanted to probe further and look into deficits in other visually guided behaviours. Due to difficulty in analysis, the amount of information obtained from an assay involving free-swimming larvae, like in the OMR assay, is limited. So, we wanted to make a stable setup for automatic stimulus delivery and reliable recording- StimUNO. The main components are an automatic stimulus delivery unit, a recording unit and an interface between these two. The stimulus delivery unit consisted of a Sony MP-CD1 mini projector connected to a laptop which runs a python code that generates the stimulus and back projects it onto a diffusion paper (Rosco 3026) affixed onto the outer wall of a 3.5 cm Petri plate (see Materials and Methods). The recording unit consists of a camera capable of high-speed recording (AVT Pike F032B ASG) fixed with an AZURE-3514MM lens and 850 nm bp filter (Azure Photonics) and an IR LED array for illumination. The camera is connected to a computer with specialised hardware for data transmission. The 2 units are connected for inter-communication by using an Arduino UNO microcontroller. The laptop from the stimulus delivery unit connects to the Arduino via its serial communication port, and the Arduino is connected to the camera using a special input cable by the manufacturer. The whole connection is such that the stimulus delivery unit sends a signal via the serial port to the Arduino while it delivers a stimulus. Then the Arduino relays it to the camera as a TTL (Transistor-transistor logic) pulse, and the camera integrates this information in the captured frame via its SIS (Secure-image Signature) feature. Figure 10.A shows the flowchart describing the working of the system.

A rough schematic of connections between the components is shown in Figure 10.B.

The SIS has to be extracted offline to get information on stimulus delivery during analysis. Since the stimulus status is directly communicated via high-speed data cables, the latency is negligible. This means that the frame with the stimulus signal is essentially the same where the larvae encounter the stimuli for the first time. Figure 10.C shows restrained larvae captured by the camera, and the SIS is zoomed in and shown.

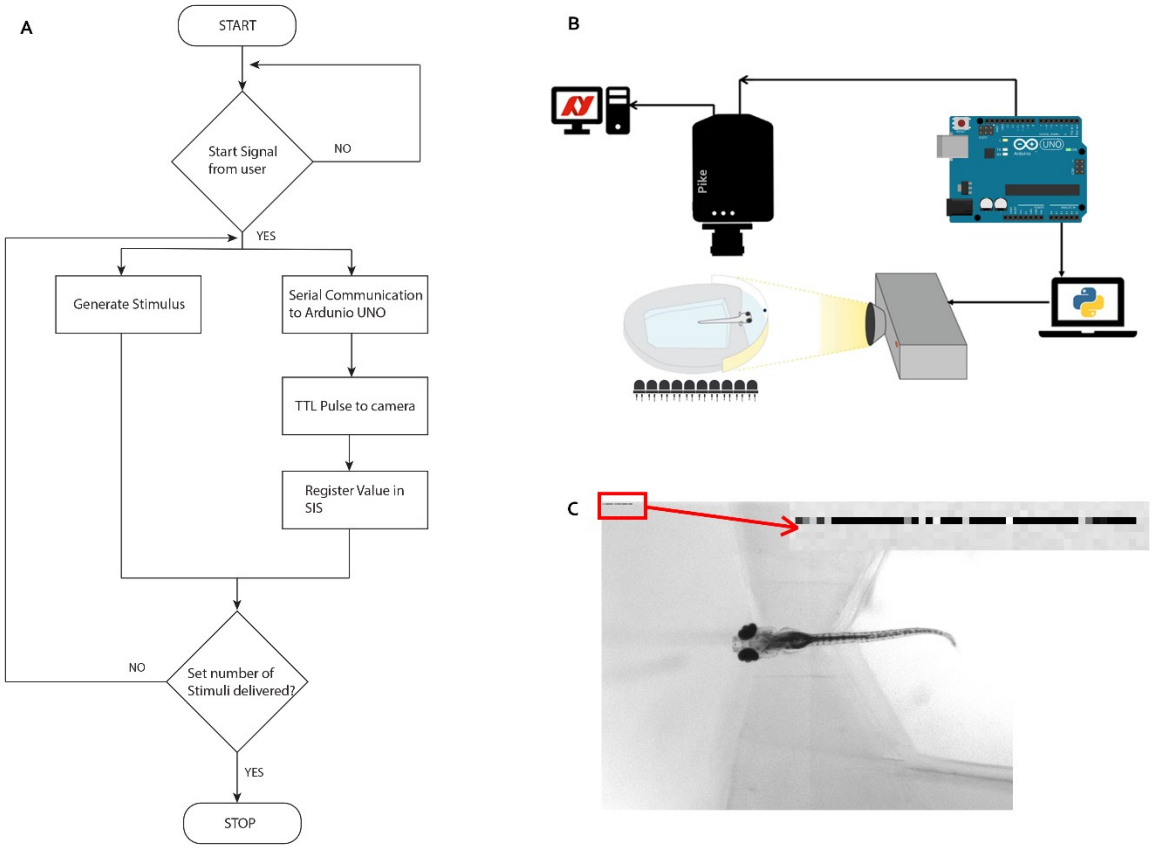


Figure 10: ***StimUNO for restrained larval experiments****. A) Flowchart on the working of StimUNO. The shapes in the flowchart follow standard conventions. B) Schematic of connections in StimUNO. C) A restrained larvae captured using the camera. The SIS is shown enlarged.*

3.3 A pipeline for automatic larval tail movement tracking using SLEAP

To extract maximum information about larval behaviour, it is essential to have an automated system for larval movement tracking. This is more relevant when recording at high frame rates, in which manual tracking is tedious and will lead to errors. We designed a pipeline for automatically tracking larval tail movements using a deep-learning-based framework SLEAP (Pereira et al., 2022). The basic workflow for training the deep learning model and using it for tracking is summarised in Figure 11.

The output from StimUNO is a series of BMP files, each corresponding to a frame of the recording. The first step is to extract the information from SIS, which is encoded in binary to human readable form, embed it in the files, and make a file containing frame identity (number) and its corresponding stimuli status. The next step will be to convert these image sequences into a video file which will be the input for SLEAP. A few videos from the collection were used to train the deep-learning model to track the larval tail accurately. The training data set was in such a way that it included recordings from both control and wild-type larvae to account for minor morphological changes associated with the mutation. For easy identification of the larvae, both the eyes and yolk sac were labelled since these were the most distinct landmarks available. The last pigmented tip of the tail was labelled for tracking the tail.

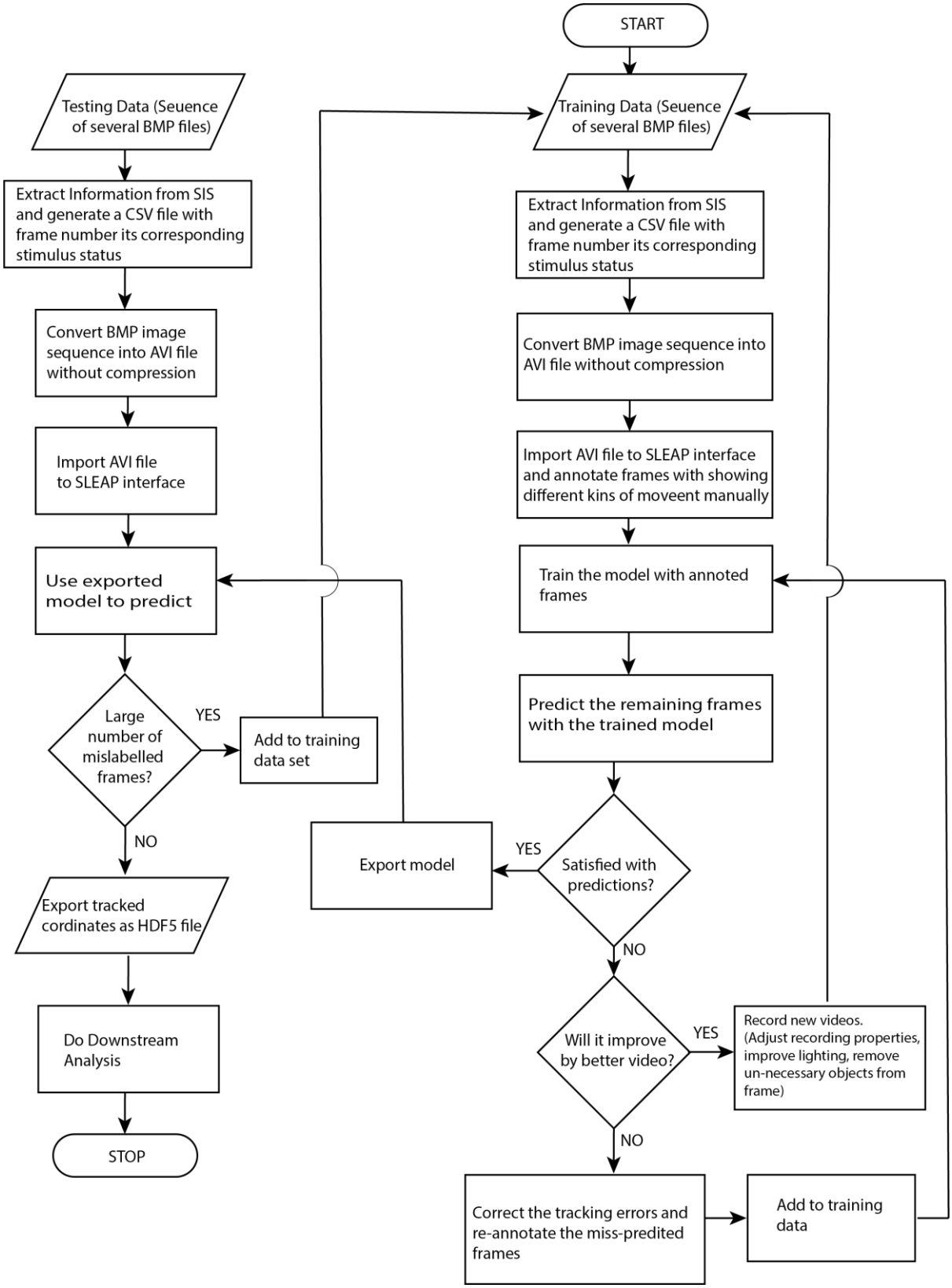


Figure 11: ***Flowchart for using SLEAP for automatic larval behaviour analysis****. The shapes used follows the standard convention.*

The model was trained with 717 frames which were manually labelled and included almost all possible tail movements within the scope of the planned experiments of both mutant and control. Figure 12 shows the tracked frames of a restrained

zebrafish larva showing various tail dynamics. The colours of the track points have been enhanced to improve visibility.

All the tracked point coordinates are exported as an HDF5 file which is then used for further analysis.

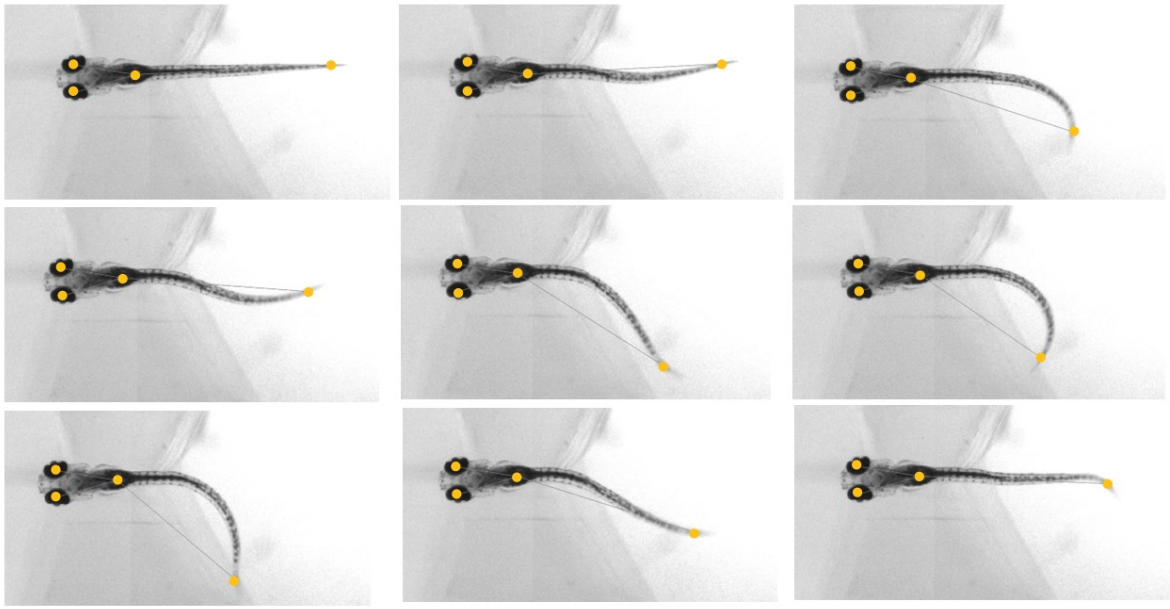


Figure 12: ***Tail tracking USING a model trained in SLEAP.*** *A representative larval tracking by SLEAP. The tracking points (yellow) have been enhanced to improve visibility. Both the eyes, the yolk sac and the tail tip are marked with yellow dots, as tracked by our SLEAP model. The photographs were taken using StimUNO.*

3.4 Automatic analysis of Eye movements using Stytra

The saccades of the eye can be tracked by fitting an ellipse around it, as shown in Figure 13 and finding the angle of its axis. An open-source package Stytra (Štih et al., 2019), does this by using traditional computer vision algorithms by thresholding the image. The ROI of the image is marked such that it is filled maximally by both eyes only and has to be marked every time for all input videos. All the tracked parameters are exported into a CSV file for further analysis.

A sample analysis of eye angles to a whole field Opto-kinetic Response (OKR) stimulus is shown in Figure 13. Since Stytra uses traditional computer vision to track eye movements, video quality is essential here, unlike tracking with SLEAP. Background disturbances should be minimised, and the video should be well-lit. Also, properly aligning the larvae in the dorsal position is important for good tracking. The shutter speed and gain of the camera are adjusted appropriately to get the best image possible.

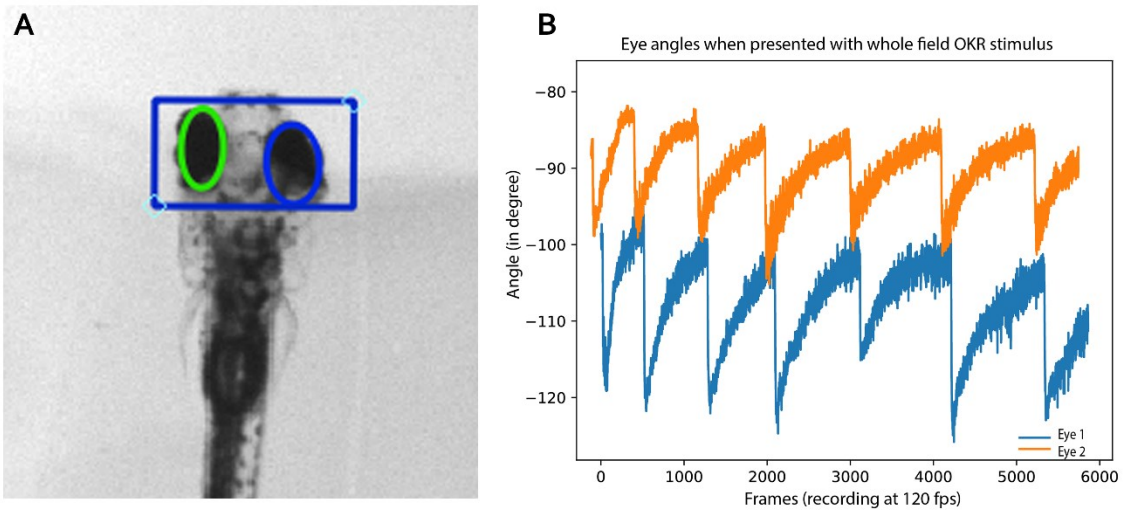


Figure 13: ***Eye tracking by using Stytra.*** *A) Marking the ROI for eye tracking. An ROI which is maximally filled with both eyes is marked in the image (blue square). Styra applies thresholding and marks 2 continuous elliptical objects in the ROI (green and blue ellipse) and tracks it across all frames. B) A representative eye tracking data when the larva is stimulated with the whole field moving grating.*

3.5 Wild-type larvae show avoidance behaviour when stimulated with a looming disc video

When a looming disc is presented to a partially restrained larva (see Materials and Methods), it perceives it as an incoming predator or a collision course and tries to move away from it. A looming disc shown as described in the material section was able to elicit a C-bend response in Wild type zebrafish larvae. Representative stages in the behaviour are shown in Figure 14.A-H. 6 out of 15 larvae showed this response when the tail movement was tracked using the model trained on SLEAP. The inter stimulus interval (ISI) was 5 s and 5 stimuli were delivered to one larva. In 5 out of 15 trials, larva responded to the first stimulus but in 1 of the trial, it responded to the second trial. When the time of response was examined for one individual larva, it was found that the first C-bend was seen 590 ms after the stimulus started. Since the dot radius increased at a rate of 82.4 px/s, in 590ms, the radius of the dot will be 48.616 px, when calibrated as discussed in the Materials and Methods section, will subtend a visual angle of 18.3^0 which matches approximately with the threshold reported ($21.7^0 \pm 2.5^0$) in Temizer et al. 2015 (Temizer et al., 2015). This is the threshold where the larva elicits a C-bend response. Though this can be evidence that we were able to elicit a looming response, more larvae need to be analysed to confirm its robustness so that it can be reliably compared against Fmn2b mutant background. Figure 14.I show the tail tip angles, which correspond to the tail movements.

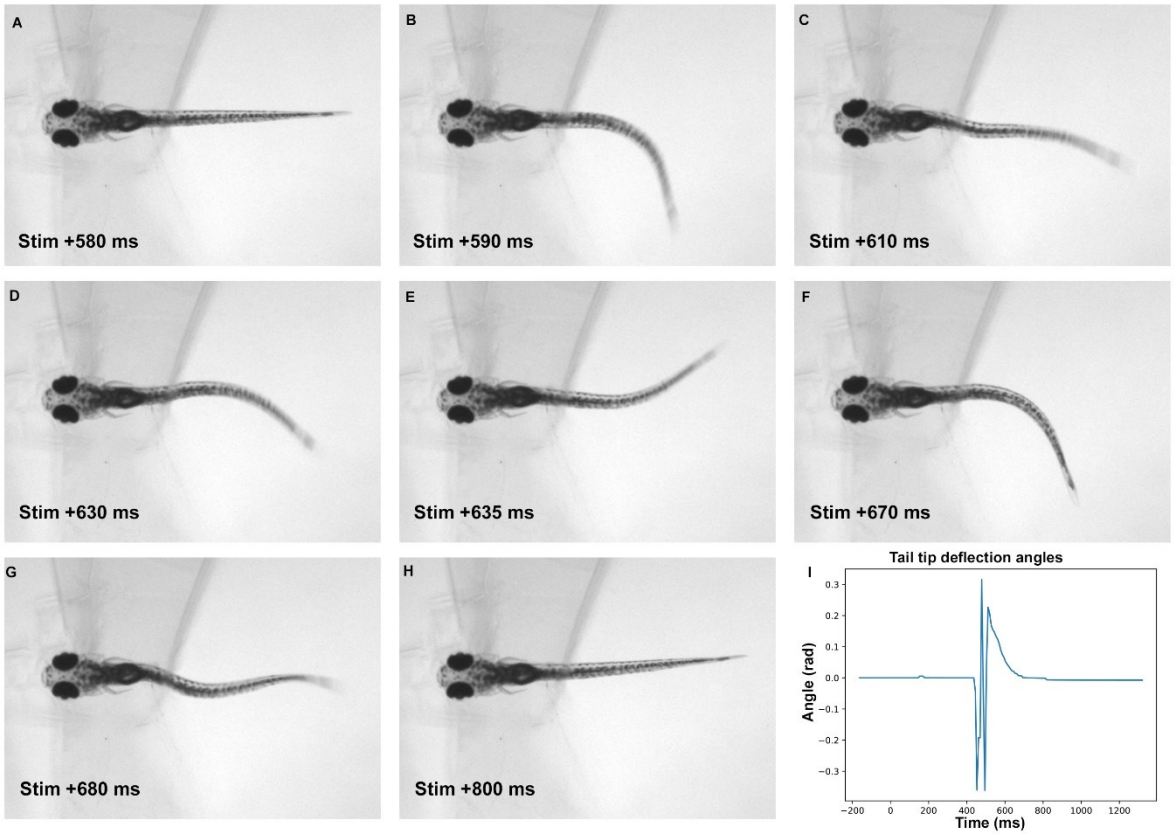


Figure 14: ***Sequence of events in a looming disc avoidance assay.*** *A- H) Larvae during different time points post-stimulus delivery. A) Larva just before C bend response. B) Larva showing the first C-bend response. C-E) Swim bouts to move away in the turned direction after the C-bend. F) Second C-bend. Swim bots to move in the turned direction. H) Larva stops tail movement. I) Tail tip deflection angle. Time point 0 is the point of stimulus delivery.*

3.6 Wild-type larvae show saccades when stimulated with whole field moving square gratings

When the restrained larva was stimulated with whole field square grating, it showed typical saccadic movements, as reported in previous studies. (Kramer et al., 2019; Matsuda and Kubo, 2021). We used StimUNO to record the larval behaviour and Stytra to track eye movements. Here, when a larva is stimulated with a whole field moving square grating, it tracks the grating and shows saccadic eye movements (see Figure 13.B). Though the behaviour is robustly shown in all of the wild-type larvae used, the accurate tracking of eye angles was a limitation in its analysis. In an ideal case, when the eye angles are available, the peaking frequency of eye angles can be quantified and used as an index to compare against the mutant background. Since Stytra uses traditional computer vision, good-quality video is necessary to get reliable data. In our case, though saccadic movements could be observed in the videos, its analysis was not performed due to the high noise in the video and the low number of good-quality videos.

3.7 Wild-type larvae elicit hunting manoeuvre when presented with a moving dot

A virtual hunting assay was set up using StimUNO, adapted from previous reports (Bianco et al., 2011). When a small moving dot was presented to a partially restrained larva (see Materials and Methods), the hunting manoeuvre involving multiple orienting turns, as reported by Bianco et al. 2011 (Bianco et al., 2011), was elicited by wild-type larvae. When the dot was on one side of the visual field of the larva, it elicited orienting J-turns to align itself towards the dot. The dot at the centre of the visual field elicited a typical capture swim response.

In our case, the response was unreliable and could not be analysed further. In more than three-fourths of the trial, the larvae exhibited no tail movement at all. Those larvae without any tail movements were not dead, as was verified by either eye movements in the recorded videos, touch-evoked response or beating heart under the microscope. Unlike the low response to repeated trials reported by Bianco et al. 2011, in our case, when the larva responded, it always responded to more than 5 out of 10 trials. An example analysis of tail movement is shown in Figure 15. In this example the interstimulus interval (ISI) was 5 s and 10 stimuli were delivered.

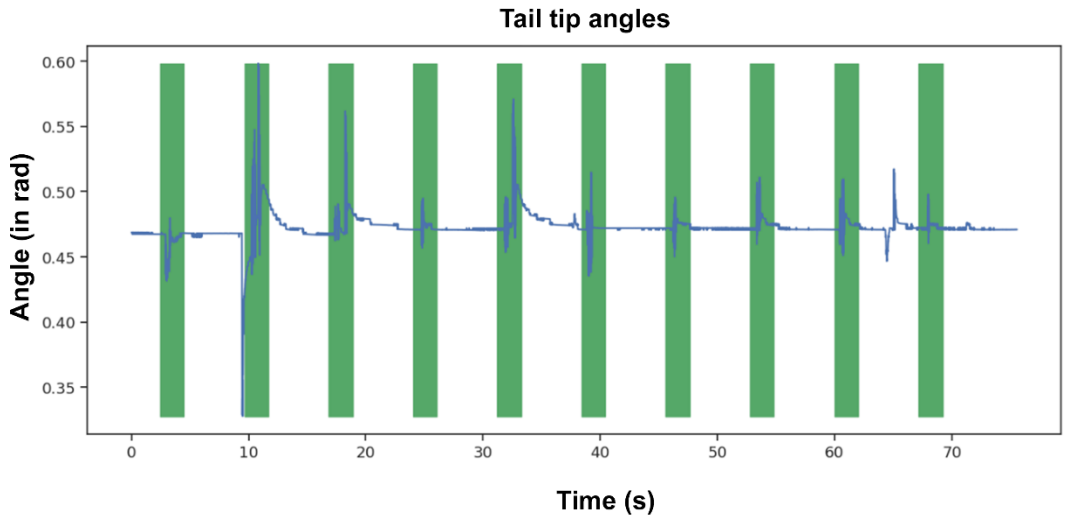


Figure 15: ***Representative tail tracking data from the virtual hunting assay****. The green-shaded region corresponds to the time at which the stimulus was presented. The angles are calculated based on a reference point in the left bottom of each frame.*

4 Discussion

As evident from the OMR assays, there is an apparent deficit in optomotor response in the case of fmn2b$^{\Delta 7/\Delta 7}$ larvae. The trends observed in the data on orientation, displacement, velocity and the fraction of larvae crossing the five-sixths of the plate suggest deficits in the optomotor response when Fmn2b is knocked out. Despite motor deficits characterised earlier (Nagar, 2021) in fmn2b$^{\Delta 7/\Delta 7}$ larvae, they could perceive the stimulus and swim in the direction of the grating. However, due to subtle errors in visual processing, they could not orient correctly. This should be tested further by looking at responses to other behaviours.

Since there has been evidence of defects at various points in the visual system, including the thinning of the optic nerve, reduction in the RGC arborisation in the tectum, and reduction in the number of inter-tectal neurons (Nagar, 2021), it would be interesting to look at other visually guided behaviours. A more extensive behaviour analysis must be done to dissect defective circuits in the fmn2b$^{\Delta 7/\Delta 7}$ larvae. The restrained larval assays developed will be useful in this regard. StimUNO and the automatic tail tracking pipeline implemented using SLEAP (Pereira et al., 2022) and eye tracking with Stytra (Štih et al., 2019) can be adapted to perform any visually guided behaviour. The tracking pipeline developed can be used in other kinds of behaviour, such as touch-evoked response, as has been implemented by lab colleagues and is not limited to zebrafish as described by developers of SLEAP (Pereira et al., 2022).

One of the limitations of automatic zebrafish larval tracking platforms, including the pipeline described in this project, is poor visibility of the animal to be tracked. An automated program can do nothing if the larvae are not visible properly on the captured frames. One way to overcome this is by including a preprocessing step that enhances the contrast of the fish against the background, but there is a limit to it. The other straightforward way is to get better cameras or improve lighting, changing shooting angles, among others.

One possible explanation for this unresponsive behaviour of larvae in many trials of the virtual hunting assay might be linked to larval handling techniques. In all the trials, the larva was reared to 7 dpf in a 10 cm Petri plate with feeding. An alternative would be to transfer it to larval growth tanks with more space to swim around. Another reason might be poor stimulus parameters. Since the parameters used were taken from previous reports (Bianco et al., 2011; Semmelhack et al., 2014), an alternative would be to use trial and error to find the proper parameters. However, since it works for some larvae, our most straightforward approach would be to improve larval handling techniques.

Since many factors affect the behaviour, including but not limited to the internal states of the animal, it is tricky to standardise behavioural assays. The parameters that worked for some researchers might not be universally applicable due to differences in instruments, environment, and fish-rearing conditions, among others.

Once we get reliable behavioural responses, it would be interesting to look at the brain activity while the larva behaves. The restrained assays developed, and StimUNO can easily be integrated with a microscope and reliably used for calcium imaging. Towards this direction, the fmn2b$^{\Delta 7/\Delta 7}$ mutant fish were crossed with a transgenic fish line which expresses a calcium sensor GCamp6f under a pan-neuronal marker. However, getting a robust behaviour response is the first step before going towards anything in that direction.

In summary, this work gives a behavioural readout of a defect in a visually guided behaviour- OMR in the fmn2b$^{\Delta 7/\Delta 7}$ zebrafish larvae and highlights the importance of Fmb2b in visually guided behaviours. We further designed and implemented an adaptable visually guided behaviour assay platform, StimUNO and made a pipeline for automatic larval behaviour tracking and analysis. This can be used as a foundation, and extensive behavioural analysis can be done to characterise different mutant zebrafish lines.

5 References

Agís-Balboa, R.C., P.S. Pinheiro, N. Rebola, C. Kerimoglu, E. Benito, M. Gertig, S. Bahari-Javan, G. Jain, S. Burkhardt, I. Delalle, A. Jatzko, M. Dettenhofer, P.A. Zunszain, A. Schmitt, P. Falkai, J.C. Pape, E.B. Binder, C. Mulle, A. Fischer, and F. Sananbenesi. 2017. Formin 2 links neuropsychiatric phenotypes at young age to an increased risk for dementia. *The EMBO Journal*. 36:2815–2828. doi:10.15252/embj.201796821.

Almuqbil, M., F.F. Hamdan, G. Mathonnet, B. Rosenblatt, and M. Srour. 2013. De novo deletion of FMN2 in a girl with mild non-syndromic intellectual disability. *Eur J Med Genet*. 56:686–688. doi:10.1016/j.ejmg.2013.10.003.

Anazi, S., S. Maddirevula, V. Salpietro, Y.T. Asi, S. Alsahli, A. Alhashem, H.E. Shamseldin, F. AlZahrani, N. Patel, N. Ibrahim, F.M. Abdulwahab, M. Hashem, N. Alhashmi, F. Al Murshedi, A. Al Kindy, A. Alshaer, A. Rumayyan, S. Al Tala, W. Kurdi, A. Alsaman, A. Alasmari, S. Banu, T. Sultan, M.M. Saleh, H. Alkuraya, M.A. Salih, H. Aldhalaan, T. Ben-Omran, F. Al Musafri, R. Ali, J. Suleiman, B. Tabarki, A.W. El-Hattab, C. Bupp, M. Alfadhel, N. Al Tassan, D. Monies, S.T. Arold, M. Abouelhoda, T. Lashley, H. Houlden, E. Faqeih, and F.S. Alkuraya. 2017. Expanding the genetic heterogeneity of intellectual disability. *Hum Genet*. 136:1419–1429. doi:10.1007/s00439-017-1843-2.

Baden, T., F. Esposti, A. Nikolaev, and L. Lagnado. 2011. Spikes in Retinal Bipolar Cells Phase-Lock to Visual Stimuli with Millisecond Precision. *Current Biology*. 21:1859–1869. doi:10.1016/j.cub.2011.09.042.

Baier, H., and M.F. Wullimann. 2021. Anatomy and function of retinorecipient arborisation fields in zebrafish. *Journal of Comparative Neurology*. 529:3454–3476. doi:10.1002/cne.25204.

Bianco, I., A. Kampff, and F. Engert. 2011. Prey Capture Behavior Evoked by Simple Visual Stimuli in Larval Zebrafish. *Frontiers in Systems Neuroscience*. 5.

Bilotta, J., S. Saszik, and S.E. Sutherland. 2001. Rod contributions to the electroretinogram of the dark-adapted developing zebrafish. *Developmental Dynamics*. 222:564–570. doi:10.1002/dvdy.1188.

Bollmann, J.H. 2019. The Zebrafish Visual System: From Circuits to Behavior. *Annual Review of Vision Science*. 5:269–293. doi:10.1146/annurev-vision-091718-014723.

Branchek, T. 1984. The development of photoreceptors in the zebrafish, Brachydanio rerio. II. Function. *Journal of Comparative Neurology*. 224:116–122. doi:10.1002/cne.902240110.

Cameron, D.A. 2002. Mapping absorbance spectra, cone fractions, and neuronal mechanisms to photopic spectral sensitivity in the zebrafish. *Visual Neuroscience*. 19:365–372. doi:10.1017/S0952523802192121.

Chemotaxis and Migration Tool | Free Software. *ibidi*.

Dreosti, E., F. Esposti, T. Baden, and L. Lagnado. 2011. In vivo evidence that retinal bipolar cells generate spikes modulated by light. *Nat Neurosci*. 14:951–952. doi:10.1038/nn.2841.

E3 medium (for zebrafish embryos). 2011. *Cold Spring Harb Protoc*. 2011:pdb.rec66449. doi:10.1101/pdb.rec066449.

Fleisch, V.C., and S.C.F. Neuhauss. 2006. Visual Behavior in Zebrafish. *Zebrafish*. 3:191–201. doi:10.1089/zeb.2006.3.191.

Geng, Y., and R.T. Peterson. 2021. Rapid Mounting of Zebrafish Larvae for Brain Imaging. *Zebrafish*. 18:376–379. doi:10.1089/zeb.2021.0062.

Kramer, A., Y. Wu, H. Baier, and F. Kubo. 2019. Neuronal Architecture of a Visual Center that Processes Optic Flow. *Neuron*. 103:118-132.e7. doi:10.1016/j.neuron.2019.04.018.

Kubo, F., B. Hablitzel, M. Dal Maschio, W. Driever, H. Baier, and A.B. Arrenberg. 2014. Functional architecture of an optic flow-responsive area that drives horizontal eye movements in zebrafish. *Neuron*. 81:1344–1359. doi:10.1016/j.neuron.2014.02.043.

Kunst, M., E. Laurell, N. Mokayes, A. Kramer, F. Kubo, A.M. Fernandes, D. Förster, M. Dal Maschio, and H. Baier. 2019. A Cellular-Resolution Atlas of the Larval Zebrafish Brain. *Neuron*. 103:21-38.e5. doi:10.1016/j.neuron.2019.04.034.

Law, R., T. Dixon-Salazar, J. Jerber, N. Cai, A.A. Abbasi, M.S. Zaki, K. Mittal, S.B. Gabriel, M.A. Rafiq, V. Khan, M. Nguyen, G. Ali, B. Copeland, E. Scott, N. Vasli, A. Mikhailov, M.N. Khan, D.M. Andrade, M. Ayaz, M. Ansar, M. Ayub, J.B. Vincent, and J.G. Gleeson. 2014. Biallelic truncating mutations in FMN2, encoding the actin-regulatory protein Formin 2, cause nonsyndromic autosomal-recessive intellectual disability. *Am J Hum Genet*. 95:721–728. doi:10.1016/j.ajhg.2014.10.016.

Leyden, C., T. Brüggemann, F. Debinski, C.A. Simacek, F.A. Dehmelt, and A.B. Arrenberg. 2022. Efficacy of Tricaine (MS-222) and Hypothermia as Anesthetic Agents for Blocking Sensorimotor Responses in Larval Zebrafish. *Frontiers in Veterinary Science*. 9.

Marco, E.J., A.B. Aitken, V.P. Nair, G. da Gente, M.R. Gerdes, L. Bologlu, S. Thomas, and E.H. Sherr. 2018. Burden of de novo mutations and inherited rare single nucleotide variants in children with sensory processing dysfunction. *BMC Med Genomics*. 11:50. doi:10.1186/s12920-018-0362-x.

Marquart, G.D., K.M. Tabor, M. Brown, J.L. Strykowski, G.K. Varshney, M.C. LaFave, T. Mueller, S.M. Burgess, S. Higashijima, and H.A. Burgess. 2015. A 3D Searchable Database of Transgenic Zebrafish Gal4 and Cre Lines for Functional Neuroanatomy Studies. *Frontiers in Neural Circuits*. 9.

Matsuda, K., and F. Kubo. 2021. Circuit Organization Underlying Optic Flow Processing in Zebrafish. *Frontiers in Neural Circuits*. 15.

Nagar, D. 2021. Formin-2b (Fmn2b) in the development of neural circuits in zebrafish. Indian Institute of Science Education and Research Pune.

Nagar, D., T.K. James, R. Mishra, S. Guha, S.M. Burgess, and A. Ghose. 2021a. The Formin Fmn2b Is Required for the Development of an Excitatory Interneuron Module in the Zebrafish Acoustic Startle Circuit. *eNeuro*. 8. doi:10.1523/ENEURO.0329-20.2021.

Nagar, D., T.K. James, R. Mishra, S. Guha, S.M. Burgess, and A. Ghose. 2021b. The Formin Fmn2b Is Required for the Development of an Excitatory Interneuron Module in the Zebrafish Acoustic Startle Circuit. *eNeuro*. 8:ENEURO.0329-20.2021. doi:10.1523/ENEURO.0329-20.2021.

Neuhauss, S.C.F. 2010. Zebrafish vision. *In* Fish Physiology. Elsevier. 81–122.

Peirce, J., J.R. Gray, S. Simpson, M. MacAskill, R. Höchenberger, H. Sogo, E. Kastman, and J.K. Lindeløv. 2019. PsychoPy2: Experiments in behavior made easy. *Behav Res*. 51:195–203. doi:10.3758/s13428-018-01193-y.

Pereira, T.D., N. Tabris, A. Matsliah, D.M. Turner, J. Li, S. Ravindranath, E.S. Papadoyannis, E. Normand, D.S. Deutsch, Z.Y. Wang, G.C. McKenzie-Smith, C.C. Mitelut, M.D. Castro, J. D'Uva, M. Kislin, D.H. Sanes, S.D. Kocher, S.S.-H. Wang, A.L. Falkner, J.W. Shaevitz, and M. Murthy. 2022. SLEAP: A deep learning system for multi-animal pose tracking. *Nat Methods*. 19:486–495. doi:10.1038/s41592-022-01426-1.

Preuss, S.J., C.A. Trivedi, C.M. vom Berg-Maurer, S. Ryu, and J.H. Bollmann. 2014. Classification of Object Size in Retinotectal Microcircuits. *Current Biology*. 24:2376–2385. doi:10.1016/j.cub.2014.09.012.

Randlett, O., C.L. Wee, E.A. Naumann, O. Nnaemeka, D. Schoppik, J.E. Fitzgerald, R. Portugues, A.M.B. Lacoste, C. Riegler, F. Engert, and A.F. Schier. 2015. Whole-brain activity mapping onto a zebrafish brain atlas. *Nat Methods*. 12:1039–1046. doi:10.1038/nmeth.3581.

Robinson, J., E.A. Schmitt, F.I. Hárosi, R.J. Reece, and J.E. Dowling. 1993. Zebrafish ultraviolet visual pigment: absorption spectrum, sequence, and localisation. *Proceedings of the National Academy of Sciences*. 90:6009–6012. doi:10.1073/pnas.90.13.6009.

Ronneberger, O., K. Liu, M. Rath, D. Rueβ, T. Mueller, H. Skibbe, B. Drayer, T. Schmidt, A. Filippi, R. Nitschke, T. Brox, H. Burkhardt, and W. Driever. 2012. ViBE-Z: a framework for 3D virtual colocalisation analysis in zebrafish larval brains. *Nat Methods*. 9:735–742. doi:10.1038/nmeth.2076.

Schindelin, J., I. Arganda-Carreras, E. Frise, V. Kaynig, M. Longair, T. Pietzsch, S. Preibisch, C. Rueden, S. Saalfeld, B. Schmid, J.-Y. Tinevez, D.J. White, V. Hartenstein, K. Eliceiri, P. Tomancak, and A. Cardona. 2012. Fiji: an open-

source platform for biological-image analysis. *Nat Methods*. 9:676–682. doi:10.1038/nmeth.2019.

Semmelhack, J.L., J.C. Donovan, T.R. Thiele, E. Kuehn, E. Laurell, and H. Baier. 2014. A dedicated visual pathway for prey detection in larval zebrafish. *Elife*. 3. doi:10.7554/eLife.04878.

Štih, V., L. Petrucco, A.M. Kist, and R. Portugues. 2019. Stytra: An open-source, integrated system for stimulation, tracking and closed-loop behavioral experiments. *PLoS Comput Biol*. 15:e1006699. doi:10.1371/journal.pcbi.1006699.

Tabor, K.M., G.D. Marquart, C. Hurt, T.S. Smith, A.K. Geoca, A.A. Bhandiwad, A. Subedi, J.L. Sinclair, H.M. Rose, N.F. Polys, and H.A. Burgess. 2019. Brain-wide cellular resolution imaging of Cre transgenic zebrafish lines for functional circuit-mapping. *eLife*. 8:e42687. doi:10.7554/eLife.42687.

Temizer, I., J.C. Donovan, H. Baier, and J.L. Semmelhack. 2015. A Visual Pathway for Looming-Evoked Escape in Larval Zebrafish. *Curr Biol*. 25:1823–1834. doi:10.1016/j.cub.2015.06.002.

Virtanen, P., R. Gommers, T.E. Oliphant, M. Haberland, T. Reddy, D. Cournapeau, E. Burovski, P. Peterson, W. Weckesser, J. Bright, S.J. van der Walt, M. Brett, J. Wilson, K.J. Millman, N. Mayorov, A.R.J. Nelson, E. Jones, R. Kern, E. Larson, C.J. Carey, İ. Polat, Y. Feng, E.W. Moore, J. VanderPlas, D. Laxalde, J. Perktold, R. Cimrman, I. Henriksen, E.A. Quintero, C.R. Harris, A.M. Archibald, A.H. Ribeiro, F. Pedregosa, and P. van Mulbregt. 2020. SciPy 1.0: fundamental algorithms for scientific computing in Python. *Nat Methods*. 17:261–272. doi:10.1038/s41592-019-0686-2.

Yoshimatsu, T., C. Schröder, N.E. Nevala, P. Berens, and T. Baden. 2020. Fovea-like Photoreceptor Specializations Underlie Single UV Cone Driven Prey-Capture Behavior in Zebrafish. *Neuron*. 107:320-337.e6. doi:10.1016/j.neuron.2020.04.021.

Zimmermann, M.J.Y., N.E. Nevala, T. Yoshimatsu, D. Osorio, D.-E. Nilsson, P. Berens, and T. Baden. 2018. Zebrafish Differentially Process Color across Visual Space to Match Natural Scenes. *Current Biology*. 28:2018-2032.e5. doi:10.1016/j.cub.2018.04.075.